Imaizumi *et al. Robomech J (2017) 4:12*
DOI 10.1186/s40648-017-0080-8

ROBOMECH Journal

RESEARCH ARTICLE

Open Access

Friction perception resulting from laterally vibrotactile stimuli

Akihiro Imaizumi, Shogo Okamoto* and Yoji Yamada

Abstract

When a human rubs a contactor that is vibrating laterally at 3–10 Hz with an amplitude of ~1 mm, the friction is perceived as being greater than that sensed when touching a stationary contactor. This phenomenon could be exploited for a new vibrotactile approach to friction perception; however, the principles behind it have yet to be explained. In this study, we hypothesized that the perceived friction increases because of the Stribeck characteristic and stick-slip phenomenon of friction, whereby the friction varies depending on the relative velocity between a subject's fingertip and contactor. The relative velocity instantaneously decreases because of the lateral vibration of the contactor, while the friction rises during the same period. To test this hypothesis, we simulated the friction forces between a fingertip and a vibrating contactor. Furthermore, we performed psychophysical experiments using five participants, in which each explored a vibrating contactor and subjectively compared the perceived friction under several stimulus conditions. The simulated friction forces, the results of the psychophysical experiments, and physical observation suggested that the transient increases in friction caused by lateral vibration of the contactor influenced friction perception for a laterally vibrating contactor.

Keywords: Friction perception, Vibrotactile stimuli, Stick-slip, Stribeck curve

Background

Friction perception is a major factor affecting our sensing of material textures. Especially, previous research intensively studied the roles of frictional vibration in the textural perception of materials when a finger is slid over a material surface [1–6]. For example, Fagiani [1] investigated the spectra of frictional vibrations where a finer surface roughness and higher sliding velocity led to higher frequency components in the spectra. Nonomura et al. [2] suggested that humans may discern different types of liquids based on the stick-slip phenomenon when they investigate fluids on flat glass.

On the other hand, in terms of the techniques used to present tactile friction, researchers have mainly used a quasi-static skin stretch on a fingertip [7–10] and electrostatic forces [11, 12]. Furthermore, texture displays using the squeeze effects caused by ultrasonic vibrations [13, 14] and surface acoustic waves [15] can reduce the perception of friction. However, there are few known methods for evoking friction perception by applying vibratory stimuli to a fingertip. A unique example may be the method proposed by Konyo et al. [16, 17] that delivered the sense of the stick-slip phenomenon by using high-frequency (250 Hz) vibrotactile stimuli. In terms of the presentation of virtual materials, vibrotactile approaches are especially effective for surface roughness (e.g., [18–22]). Moreover, the vibrotactile stimuli are used for hardness [23–26] and softness [17, 27–29] presentation, respectively, in tapping and pushing the object surface. However, thus far, few researchers have attempted to deliver the frictional characteristics in sliding on the surface using the vibrotactile stimuli.

Recently, we have observed that the perception of friction can be presented by a vibrotactile approach that is completely different from those previously proposed [30]. When a fingertip is slid over a flat plate that is vibrating asymmetrically at several Hz in a tangential direction, the perception of friction depends on the direction of the finger movement. When the finger moves in one direction, the perceived friction and

*Correspondence: okamoto-shogo@mech.nagoya-u.ac.jp
Department of Mechanical Sicence and Engineering, Nagoya University, Nagoya, Japan

Springer Open

© The Author(s) 2017. This article is distributed under the terms of the Creative Commons Attribution 4.0 International License (http://creativecommons.org/licenses/by/4.0/), which permits unrestricted use, distribution, and reproduction in any medium, provided you give appropriate credit to the original author(s) and the source, provide a link to the Creative Commons license, and indicate if changes were made.

the impulse of the friction force are larger than those observed when the finger is slid in another direction. We believe that this phenomenon is caused by the occurrence of sticking between the finger pad and the vibrating material, depending on the direction of movement of the finger. Similarly, an increase in the perception of friction arises between a subject's fingertip and a symmetrically vibrating plate [31]. These tangential vibrations induce a sense of sticking at low frequencies between the fingertip and material, and barely cause a sense of vibration or any perceived change in the surface texture when the surface is smoothly scanned. As a result, the vibrating plate is felt like a material that frequently causes a fingertip to be stuck while sliding. Despite these demonstrations, the perception of friction via a tangentially vibrating plate has yet to be explained. In this study, with the ultimate goal of devising a more effective friction display, we devised a principle based on an investigation of the effects of the parameters of vibrotactile stimuli on the perception of friction from the aspects of physical simulation and the results of psychophysical experiments on perceived friction in conjunction each of which is limited to corroborate the hypothesized principle.

Hypothetical principle: friction perception via lateral vibration

As shown in Fig. 1, a fingertip is assumed to slide at a constant velocity on a contactor that is vibrating in a tangential direction. Owing to the friction with the contactor, the finger pad deforms in the shear direction, and then friction is perceived. The positions of the finger pad and contactor are denoted by $x_p(t)$ and $x_c(t)$, respectively. The contactor vibrates sinusoidally:

$$x_c(t) = A \sin \omega t \tag{1}$$

where A and ω are the amplitude and angular frequency, respectively, of the contactor. Focusing on the relative velocity between the finger pad and contactor ($\dot{x}_p(t) - \dot{x}_c(t)$), we hypothesized the following two principles by which a greater degree of friction is perceived by sliding a fingertip over a tangentially vibrating contactor, rather than over a stationary contactor.

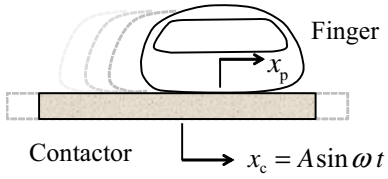

Fig. 1 Finger sliding over laterally vibrating contactor

Vibrotactile stimulus causes stick and slip phenomenon to give rise to greater perception of friction

As shown in Fig. 2, the sign of $\dot{x}_p(t) - \dot{x}_c(t)$ switches when the velocity of the vibrating contactor exceeds the velocity of the finger. At that instant, the fingertip and contactor stick to each other, and static friction arises. On the other hand, for a stationary contactor, $\dot{x}_p(t) > \dot{x}_c(t) = 0$ is true, and the kinetic friction becomes dominant. Because the static friction is larger than the kinetic friction, the vibrating contactor would produce the greater perception of friction.

Vibrotactile stimulus produces small relative velocity to give rise to greater perception of friction

Figure 3 shows the relative velocity and friction when the velocity of the contactor is constantly smaller than that of the finger: $\dot{x}_c(t) < \dot{x}_p(t)$. In such a case, the relative velocity does not become zero. As shown in Fig. 3 (right), the friction continuously changes with the relative velocity, according to the Stribeck curve. When the relative velocity is minute, the friction coefficient is large owing to the contact between the microscopically rough surfaces. The friction coefficient subsides, however, as the relative velocity increases. In the latter part of this paper, we describe an experiment to demonstrate the friction characteristics between a fingertip and the plastic plate we used in the experiment. As a result, the friction of the vibrating contactor (solid curve in Fig. 3, bottom) far exceeds that of the stationary contactor (dotted line in Fig. 3, bottom).

Apparatus

We used the vibration presentation system shown in Fig. 4. A finely polished ABS plastic contactor was driven by a DC motor (RE-40, Maxon Motor, Switzerland), the rotational speed of which was reduced by 1/2 through a timing pulley-belt mechanism. The position of the

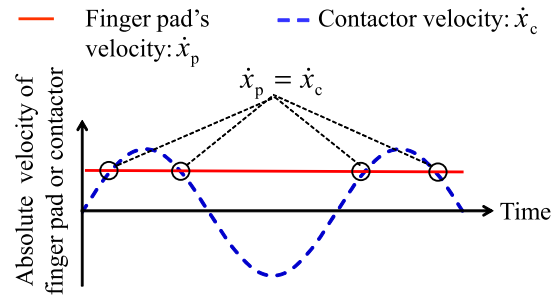

Fig. 2 Velocities of finger and vibrating contactor. The contactor (*dotted line*) sinusoidally vibrates whereas the finger velocity (*solid*) is constant. At those points at which $\dot{x}_p - \dot{x}_c$ becomes zero, static friction arises

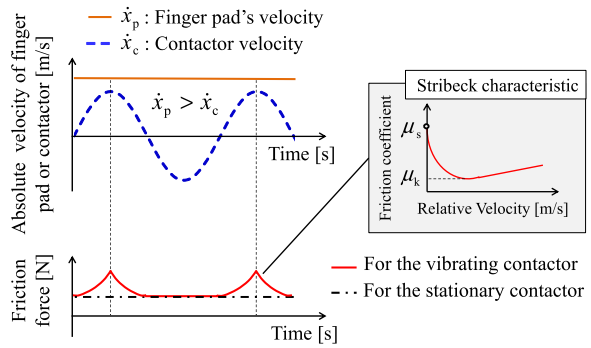

Fig. 3 Velocities of fingertip and vibrating contactor when $\dot{x}_p > \dot{x}_c$. *Bottom* Friction forces between the finger and contactor. The friction depicted by the *red curve* increases as the relative velocity becomes minute. *Right* Stribeck characteristic of friction, where μ_s and μ_k are the static and kinetic friction coefficients, respectively

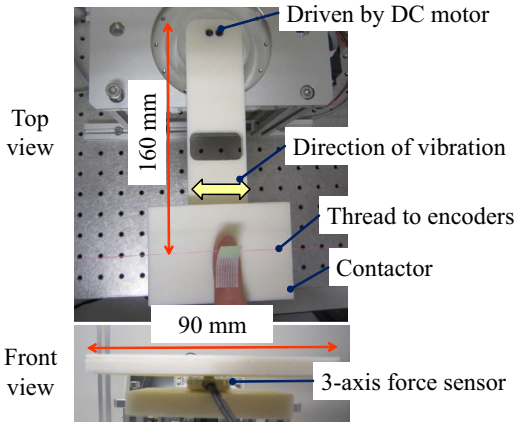

Fig. 4 Lateral vibrotactile display with a three-axis force sensor. Two encoders (not shown) measured the fingertip position by being attached to a thread taped to the finger nail

contactor ($x_c(t)$) was measured by an encoder (Type L, Maxon Motor, nominal resolution: 7.67E-4 rad) installed on the DC motor. The contactor was designed to be light but with a suitably large sliding range (90 mm). A three-axial force sensor (USL08-H18-1KN-AP, Tech Gihan, Japan) was located beneath the contactor to record the tangential and normal components of the interaction force between the fingertip and the contactor.

The position of the fingertip ($x_f(t)$) was calculated based on a triangulation method using two encoders (RE-30E-500-213-1, NIDEC COPAL ELECTRONICS Corp., Japan, resultant position resolution: 0.010 mm) which were connected by a string taped to the subject's finger nail. Each encoder was installed on a pillar set left or right side the vibrotactile display such that these two encoders and fingertip were aligned. The string was tensioned by a weight at each side and was wound by the encoders by way of pulleys. We should note that this method measured the position of the finger nail, and the finger pad further deforms in lateral direction.

To achieve a sinusoidal vibration, the motion of the contactor was feedback-controlled by linear quadratic control with the integration (LQI) method. This computer-control and sampling of the position and force were all performed at a frequency of 1 kHz. This apparatus was used for the measurement of friction and the psychophysical experiments described in sections "Simulation of friction phenomena between vibrating contactor and sliding fingertip" and "Psychophysical experiment addressing friction perception resulting from laterally vibrotactile stimuli", respectively.

Simulation of friction phenomena between vibrating contactor and sliding fingertip

As mentioned previously, we tested our hypothesis by examining the simulated friction and human psychophysical responses. Here, we describe the simulation of the frictional behavior of a fingertip that is sliding on a vibrating contactor.

Physical model

We used the physical model shown in Fig. 5 where the finger pad is connected to the bone by way of a spring and damper. The left and right figures are equivalent expressions. This one degree of freedom (1-DOF) model can be applied at least within a limited range of normal load for the tangential deformation of the finger pad [32, 33].

Let x_p, m, c, and k denote the displacement of the finger pad, the equivalent mass, viscosity, and spring constant of the finger pad, respectively. The equation of motion is then given as

$$\begin{aligned} &m\ddot{x}_p + c(\dot{x}_p - \dot{x}_f) + k(x_p - x_f) \\ &\quad = -\mathrm{sgn}(\dot{x}_r) f_r(t) \end{aligned} \tag{2}$$

where $\dot{x}_r(t) = \dot{x}_p(t) - \dot{x}_c(t)$ and $f_r(t)$ are the relative velocity between the finger pad and contactor and the friction force, respectively. The motion of the contactor

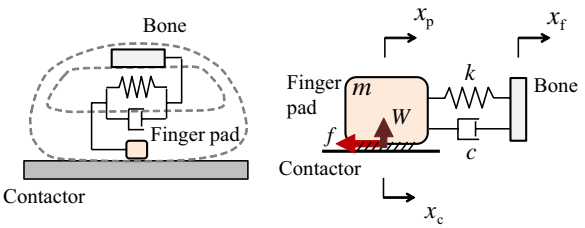

Fig. 5 Physical model of friction between fingertip and contactor. These two models are equivalent

was determined by a sinusoidal function (1). Because the human hand force is regarded as being large enough to maintain the intended motion, the motion of the finger is given by $\dot{x}_f(t) = \text{constant}$, and $\ddot{x}_f(t) = 0$.

The Stribeck curves for the skin friction have previously been reported in the literature [34–36]. As described above, by assuming the frictional characteristic between the fingertip and contactor to be a Stribeck curve, thus following the typical equation for a Stribeck curve, the friction coefficient can be modeled as

$$\mu(W, \dot{x}_r(t)) = \mu_k + (\mu_s - \mu_k) \exp\left(-a\frac{\dot{x}_r(t)}{W}\right) + b\frac{\dot{x}_r(t)}{W} \tag{3}$$

where μ_s, μ_k, and W are the static and kinetic friction coefficients and the normal load of the finger, respectively. Two constants, a and b, specify the profile of the curve. The friction force is determined by

$$f_r(t) = \mu(W, \dot{x}_r(t))W. \tag{4}$$

In (2) and (3), we used the relative velocity between the finger pad and contactor $\dot{x}_r(t) = \dot{x}_p(t) - \dot{x}_c(t)$ to determine the friction, whereas the measured friction referred the relative velocity between the finger bone and contactor. In general, measurement of the deformation of the finger skin that is sliding on a surface is not easy, and we could not experimentally acquire the true relative velocity between the finger pad and contactor $\dot{x}_p(t) - \dot{x}_c(t)$. Therefore, we defined the experimentally measured friction as a function of $\dot{x}_f(t) - \dot{x}_c(t)$ as described in section "Specification of friction parameters". In the simulation, these two types of relative velocities are largely the same in terms of their magnitudes while a phase difference exists between them, which indicates that the magnitude of simulated friction forces does not substantially change using either type of relative velocity.

Specification of friction parameters

We determined the parameters μ_s, μ_k, a, and b in (3) based on an experiment in which a fingertip was slid on a vibrating contactor. The contactor was vibrated at 6 Hz with an amplitude of 1.25 mm. After the fingertip was wiped with a dry cleaning tissue, it was used to repeatedly scan the non-lubricated contactor (which has also been wiped with a tissue a priori) in one direction for 120 s with the indicated normal load being 1 N. During this period, the contactor was scanned approximately 100 times. Using valid samples that satisfied 0 N $< f_r$ and 0.4 N $< W$, f_r/W values were plotted as a function of $(\dot{x}_f - \dot{x}_c)/W$, as shown in Fig. 6. The f_r/W values varied continuously with changes in the $(\dot{x}_f - \dot{x}_c)/W$ values.

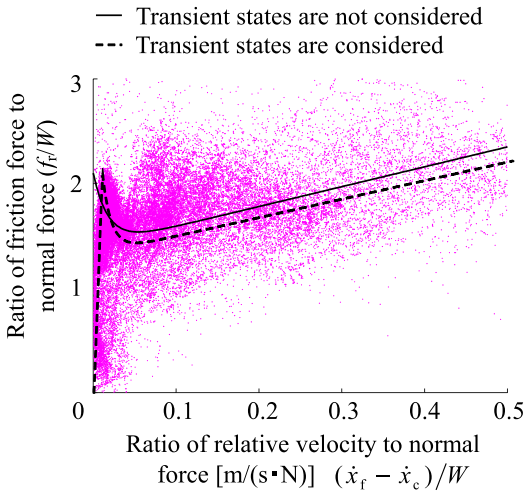

Fig. 6 Friction characteristic between contactor and finger. The *solid line* is the characteristic of maximum static friction and kinetic friction. The *dotted line* is the characteristic considering the transient states of the static friction

Using $\dot{x}_f - \dot{x}_c$ instead of $\dot{x}_r = \dot{x}_p - \dot{x}_c$, these samples were fitted to (3) by the application of the least-squares method. The solid curve in Fig. 6 shows an approximated curve ($\mu_s = 2.1$, $\mu_k = 1.4$, $a = 55$, $b = 1.9$, $R^2 = 0.91$), which indicates that the static friction rapidly decreases at smaller relative velocities whereas the friction gradually increases at greater $(\dot{x}_f - \dot{x}_c)/W$ values.

Although the above relates to the friction arising when a fingertip is slid on a vibrating contactor, we also observed a similar friction curve for sliding on a stationary contactor. Also, the figure shows the samples collected from one of the five participants, those for the other participants exhibited similar curves with their average and standard deviations of friction coefficients being $\mu_s = 2.1 \pm 0.2$ and $\mu_k = 1.3 \pm 0.2$.

Friction model with pre-maximum-static friction

The solid curve does not successfully express smaller f_r/W values at small $(\dot{x}_f - \dot{x}_c)/W$ values. This is because Fig. 6 also includes the static friction before it reaches the maximum static friction force. Such a transient region is not considered by (3). We used another equation to model this region as a linear function, which is

$$\mu(\dot{x}_r, W) = \begin{cases} p\frac{\dot{x}_r}{W} & \text{for}\left(\frac{\dot{x}_r}{W} < d\right) \\ \mu_k + (\mu_s - \mu_k) & \exp\left\{-a\left(\frac{\dot{x}_r}{W} - d\right)\right\} \\ +b\left(\frac{\dot{x}_r}{W} - d\right) & \text{for}\left(d \le \frac{\dot{x}_r}{W}\right) \end{cases} \tag{5}$$

where d is a value at which to switch between the two equations. When $\dot{x}_r/W < d$, f_r/W is a linear function of $\dot{x}_r/W$ which reaches a maximum static friction at $\dot{x}_r/W = d$. In the same way as for the previous equation, we also specified the parameters using the least-squares method ($p = 400$, $d = 0.005$, $\mu_s = 2.1$, $\mu_k = 1.4$, $a = 86, b = 2.0$, $R^2 = 0.93$). The resulting curve is indicated by the dotted line in the figure.

In these two types of fitting, many samples fell far from the fitted curves. One plausible reason for these variations is that, in the case of an elastic object such as a finger pad, the friction varies nonlinearly with the normal load [37, 38], which was not addressed by our model equations. Moreover, the transition of a fingertip's frictional state from stuck to slipping appears to be largely probabilistic, such that a stuck fingertip area either smoothly or non-continuously decreases to zero at random [39]. Unfortunately, it is demanding to incorporate these factors because there is no widely accepted models of the varying finger load during tactile exploration and probabilistic frictional behaviors for human fingertip.

Simulation of friction

In the simulation of friction described below, we used the abovementioned two equations, (3) and (5), and arrived at the same conclusions in terms of the order of the maximum and average friction forces. Here, therefore, we explain the friction forces as simulated using (3) (solid line in Fig. 6).

Table 1 lists the values of the parameters in (2) and (3) used in the simulation of friction. The mechanical parameters for the fingertip were set to the average values reported by Wiertlewski and Hayward [32] who estimated the parameters for the shear displacements caused by shear forces. The finger velocity $\dot{x}_f$ was determined such that we could test the two types of hypotheses described in section "Hypothetical principle: friction perception via lateral vibration". When $\dot{x}_f = 0.1$ m/s, $\dot{x}_r(t) > 0$ continues to apply, whereas when $\dot{x}_f = 0.04$ m/s, $\dot{x}_r(t)$ periodically falls to zero with some of the stimulus conditions. These finger velocities are within the range of the natural texture exploration [40–42].

Table 1 Parameters used for simulation

Symbol	Meaning	Value
m (kg)	Mass of finger pad	1.0×10^{-4}
k (N/m)	Stiffness	1.0×10^{3}
c (N·s/m)	Viscosity	1.0
μ_s	Static friction coefficient	2.1
μ_k	Kinetic friction coefficient	1.4
a	Constant coefficient	55
b	Constant coefficient	1.9
W (N)	Normal force	1.0
$\dot{x}_f$ (m/s)	Finger velocity	0.1 or 0.04

Table 2 lists the vibratory stimulus conditions used in the simulation. By varying the vibratory frequency and amplitude, we were able to simulate several different friction conditions. We also used these stimulus conditions in the later psychophysical experiments. Due to the stability issue of the control system, the highest frequency that we tested was set to 9 Hz.

Figure 7 (top) shows the simulated friction for each stimulus condition when $\dot{x}_f = 0.1$ m/s and $\dot{x}_r(t) > 0$. With the exception of the friction on the stationary contactor, the friction forces vary with the changes in the relative velocity. They reach a maximum when the relative velocities are the smallest. The stimulus conditions clearly influence the simulated friction. The order of the maximum friction forces is #4 > #3 > (#2, #1) > #0. This order corresponds to that of the maximum velocities of the vibratory stimuli. The friction with stimulus #4, which has the highest frequency and velocity, was the highest. On the other hand, that for the stationary contactor was the smallest among the five types of stimulus conditions. The orders of the average friction over time are the same as those of the maximum friction; however, there differences are minute. The average forces are 1.62 N for #4, 1.60 N for #3, and 1.59 N for #3, #2, and #1. The simulated friction suggests that the order of the perceived frictions will also be similar. We discuss which of the average or transient deviation of friction forces are perceptually effective in section "Effects of transient changes in friction forces caused by lateral vibration on friction perception".

Figure 7 (bottom) shows the simulated friction when $\dot{x}_f = 0.04$ m/s, for which the relative velocity may periodically fall to zero, and the finger pad and contactor stick to each other. For stimuli #4 and #3, sticking occurs and the friction reaches the maximum static friction when $\dot{x}_r(t) \to +0$. The contactor then passes by the finger when $\dot{x}_r(t) < 0$, and the direction of the tangential force changes. On the other hand, only kinetic friction acts for the other stimulus conditions. Given that the static

Table 2 Vibratory stimuli used in the simulation and psychophysical experiments

Stimulus #	Frequency (Hz)	Amplitude (mm)	Maximum velocity of contactor (m/s)
#0	0	0	0
#1	3	1.25	0.024
#2	6	0.625	0.024
#3	6	1.25	0.048
#4	9	1.25	0.072

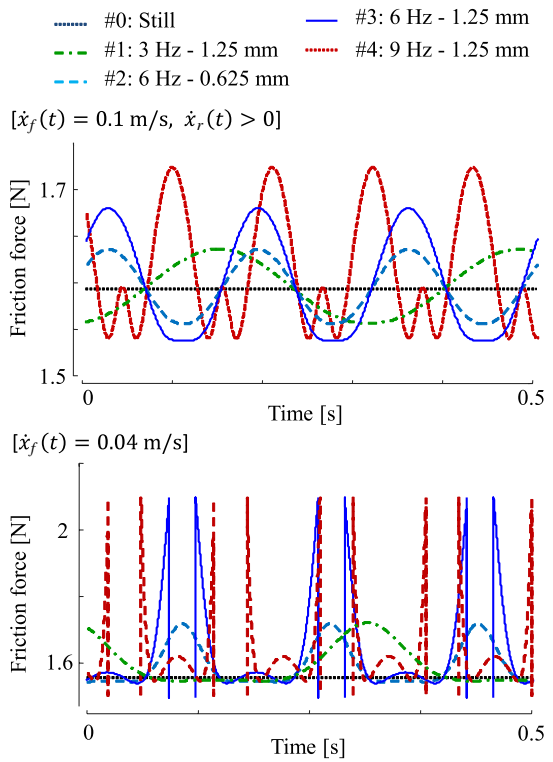

Fig. 7 Temporal course of simulated friction forces caused by vibrotactile stimuli. *Top* When $\dot{x}_f = 0.1$m/s and $\dot{x}_r(t) > 0$ constantly apply. *Bottom* When $\dot{x}_f = 0.04$ m/s and $\dot{x}_r(t)$ can be zero. For stimuli #3 and #4, the simulated friction forces are not continuous because the direction of the friction force is not always the same as that of the finger velocity

friction force is perceptually prominent, the order of the perceived friction may be $(\#4, \#3) > (\#2, \#1) > \#0$.

Psychophysical experiment addressing friction perception resulting from laterally vibrotactile stimuli

The experimental protocol was approved by the institutional review board of the School of Engineering, Nagoya University.

Methods

We investigated the friction perceived when touching a laterally vibrating contactor by applying Scheffe's paired comparison. After wiping his/her finger pad with a cloth, each participant touched the contactor in the non-lubricated condition. The participants wore headphones through which pink noise could be heard, and also wore an eye mask, thus shutting out auditory and visual cues, respectively. The participants tested each of the paired stimuli for 10 s, and then he or she judged which stimulus gave the greater sensation of friction using a 7-step scale (−3: The 1st stimulus was felt to have the greater degree of friction, 0: The two stimuli were felt to have the same degree of friction, +3: The 2nd stimulus was felt to have the greater degree of friction).

As described below, each participant repeated the above-mentioned procedure 20 times to compare the five types of stimuli for each of the two finger velocities. Hence, in total, each participant performed 40 trials. The reference velocity levels were 0.1 and 0.04 m/s, which were also used in the previously described simulation. For each velocity level, each participant could scan the contactor 17–18 and 7–8 times, respectively, within 10 s on average. The participant practiced these hand velocities before the experiment. Furthermore, the finger velocity was monitored during the experiment. If the velocity was deemed to be significantly larger or smaller than the nominal value during a trial (more than twice as large or less than half, approximately), the experimenter instructed the participant to correct the velocity, after which the trial was repeated. The finger load normal to the contactor was maintained at approximately 1 N, which again was attained by pre-trial practice and subsequent monitoring.

Participants

Five university students, who had responded to an in-house advertisement, participated in the experiment after signing an informed consent document. None of them had substantial injuries to their hands and none reported any perceptual impairment. They were unaware of the objectives of the study before the experiment.

Stimuli

The five types of stimulus conditions listed in Table 2, which were also used in the simulation, were used in the experiment. For these five conditions, ten pairs were configured. These pairs were presented in random order as a single set, and two sets were performed for each combination of participant and finger velocity.

Results

Amplitudes of vibrating contactor

When the finger pad was in contact with the contactor ($W > 0.01$ N), the means and standard deviations of the amplitudes of the vibrating contactor were 1.26 ± 0.15, 0.65 ± 0.12, 1.26 ± 0.18, and 1.27 ± 0.22 mm, for stimuli #1, #2, #3, and #4, respectively, all of which are close to the set values of 1.25 or 0.625 mm.

Ranks of perceived friction

We calculated the ratings assigned to the stimuli based on Scheffe's method [43], and then tested the ranks of the perceived friction by applying the Steel-Dwass test.

The ranks of the perceived friction for the stimuli when the finger velocity was 0.1 m/s and $\dot{x}_r(t) > 0$ are shown in

Fig. 8. The small dots are the ranks reported by the individuals, and the diamonds are their averages. The perceived degrees of friction for stimuli #4 and #3 were the largest, followed by those for stimuli #2 and #1. The friction perceived with the stationary contactor (stimulus #0) was the lowest. Especially, four of the five participants agreed that stimulus #4 produced the largest perceived friction, and all agreed that stimulus #0 produced the lowest perceived friction. The figure also shows the maximum values of the simulated friction (filled circles) for the five stimulus conditions. These rankings of the stimuli are consistent between the psychophysical experiment and the simulations. As mentioned above, the rankings were the same for the simulated maximum and average friction.

Figure 9 shows the rankings of the perceived friction when $\dot{x}_f = 0.04$ m/s and $\dot{x}_r(t)$ could be zero. The friction perceived with stimuli #4 and #3 were larger than those perceived with the others. Stimuli #2 and #1 followed them and stimulus #0 (stationary contactor) produced the smallest perceived friction. The large perceived friction produced by #4 and #3 could have resulted from the static friction and frequent sticking between the finger pad and contactor, as indicated by the simulation. When the intended finger velocity was 0.04 m/s, the results of the psychophysical experiments and the simulation are also consistent.

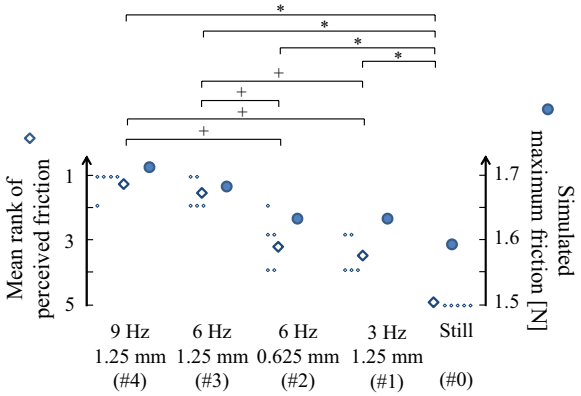

Fig. 8 Order of perceived friction and value of maximum simulated friction when $\dot{x}_f = 0.1$m/s and $\dot{x}_r(t) > 0$. *p < 0.05, $^{+}$p < 0.10 (Steel-Dwass test). The smaller dots signify the ranks reported by the individuals, while the *larger diamonds* signify the mean ranks for all the participants

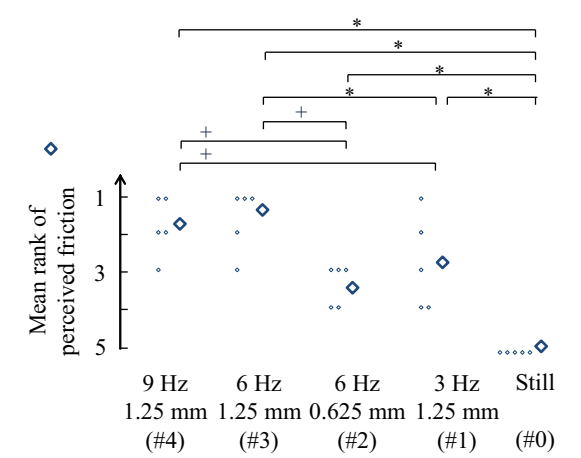

Fig. 9 Order of perceived friction when $\dot{x}_f = 0.04$ m/s and $\dot{x}_r(t)$ can be zero. *p < 0.05, $^{+}$p < 0.10 (Steel-Dwass test). The *smaller dots* signify the ranks reported by the individuals, while the *larger diamonds* signify the mean ranks for all the participants

Mean and deviations of friction forces and coefficients of friction

Figure 10 (top) shows the average friction forces computed from the samples obtained from all the participants and trials when $W > 0.01$ N. The average friction forces for those conditions with large stimulus numbers were basically larger than those with small stimulus numbers. The rankings for the average friction forces were found to be comparable to those obtained for perceived friction, as shown in Figs. 8 and 9. Nonetheless, the largest difference in the average friction forces among the stimulus conditions was only approximately 0.1 N, and the differences were not statistically significant ($p = 0.625$ and 0.570 for $\dot{x}_f = 0.1$ and 0.04 m/s, respectively) by two-way ANOVA with the participants and stimulus conditions being factors. The friction forces significantly varied between individuals ($p < 0.001$ for two types of velocity levels).

Figure 10 (middle) shows the standard deviations of the friction forces during the scanning motion. In order to evaluate the transient change in the friction caused by the lateral vibration of the contactor, for each trial, the standard deviation was computed after being high-pass-filtered with the cutoff frequency being 2.5 Hz. With this operation, low-frequency deviations of friction originated from the human hand motion were removed. The standard deviations were then averaged for individual participants. These values prominently present the effect of vibration with greater values for larger stimulus numbers, which can be graphically seen in section "Temporal course of friction and velocity". Two-way ANOVA indicated that the deviations of friction were significantly different among the stimulus conditions ($p = 0.001$ for $\dot{x}_f = 0.1$ and 0.04 m/s). These transient changes in friction caused by the vibrated contactor might have led to the sense of sticking as discussed in section "Effects of transient changes in friction forces caused by lateral vibration on friction perception".

Figure 10 (bottom) also shows the average coefficients of friction for each stimulus condition. The coefficients

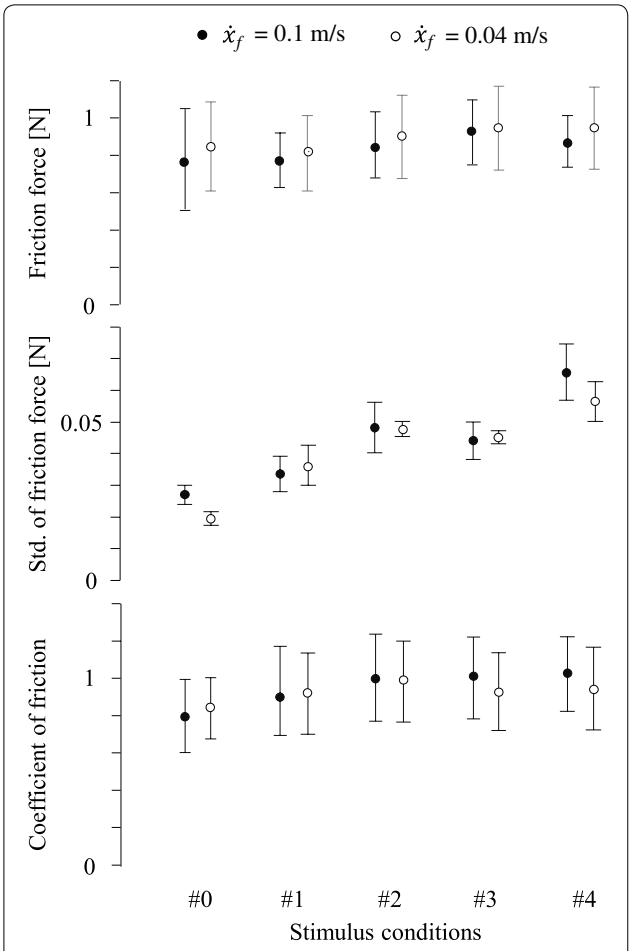

Fig. 10 Averages and standard deviations of friction forces and apparent coefficients of friction among all of the participants. *Error bars* are the standard deviations among the participants

were calculated as the ratio of the tangential force to the load W. The average coefficients were significantly different among the stimulus conditions for both velocity levels ($p < 0.01$, two-way ANOVA). Those coefficients for stimuli #1–#4 where the contactor vibrated and caused the variation of friction were greater than those for stimulus #0 that was a stationary condition. In contrast, the coefficients appeared approximately equal for stimuli #1 –#4.

Decrease in relative velocity

A decrease in the relative velocity between the finger and the contactor is a barometer to check the effect of the vibrated contactor. For each trial, we calculated the period at which the relative velocity was below 40% of the intended finger velocity. The 40% corresponds to 0.04 of 0.1 m/s, and the Stribeck curve that was used in this study reaches the bottom around this velocity.

Table 3 Percentage period where $\dot{x}_f - \dot{x}_c < 0.4 \cdot \dot{x}_f$ during the contact period. Mean and standard deviation values among the participants

$\dot{x}_f$	Stimulus number				
	#0	#1	#2	#3	#4
0.04	5 ± 3	10 ± 4	10 ± 5	22 ± 6	23 ± 5
0.1	5 ± 3	8 ± 4	8 ± 3	15 ± 4	21 ± 5

Table 3 summarizes the ratio of the period to the contact period at which $W > 0.01$ N. These values are the mean and standard deviations among the participants for each stimulus condition. Because of the imperfect control of the exploring velocity, the relative velocities were below 40% of the intended finger velocities for approximately 5% of the contact time even under non-vibratory condition (#0). In general, decreases in the relative velocity were observed for longer periods as the stimulus number increased for the intended finger velocity of 0.1 m/s ($p < 0.01$, two-way ANOVA) and 0.04 m/s ($p < 0.01$, two-way ANOVA). These observations indicate that the relative velocities were lowered by the lateral vibration of the contactor as we designed. The principles hypothesized in section "Hypothetical principle: friction perception via lateral vibration" imply that the lowered relative velocities raised the friction forces.

Temporal course of friction and velocity

Figure 11 shows samples of the interaction forces between the fingertip and contactor, together with their velocities. The fingertip slid on the contactor when the finger velocity and normal force were positive because the participant repeatedly scanned it in the same direction. The finger velocity and normal load naturally varied under the instruction for unifying them. Also, the sinusoidal motion of the contactor was moderately maintained with the disturbance of human finger force.

The left-hand figure shows a sample for which the intended finger velocity was 0.1 m/s and greater than that of the contactor. The velocity of the finger relative to the contactor was always larger than zero during touch.

The right-hand figure shows a sample for which the intended finger velocity was 0.04 m/s, which more closely approximated to that of the contactor. Under this condition, the relative velocity was supposed to occasionally fall to zero, and sticking occurred in sync with the contactor vibration that was associated with instantaneous increase in the friction force. Unfortunately, as mentioned before, since we could not measure the actual relative velocity between the finger pad and vibrating contactor, we may

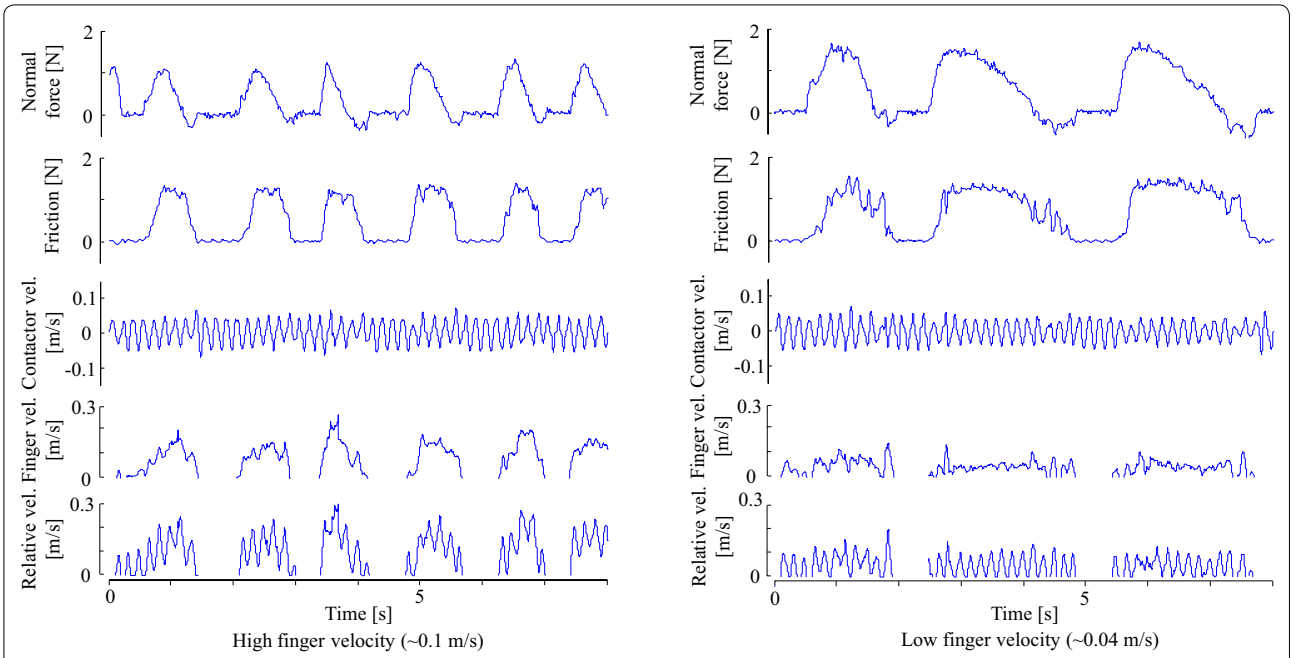

Fig. 11 Temporal course of physical quantities observed during experiments. *Left* Those when the intended finger velocity was 0.1 m/s and the relative velocity was constantly positive while touching the contactor. *Right* Those when the intended finger velocity was 0.04 m/s. Stimulus condition was #2 for which the frequency and amplitude were 6 Hz and 0.625 mm, respectively. While the normal force was nearly zero, the finger was not touching the contactor and the finger velocity is not shown. Because the finger movement was reciprocating, its velocity was alternately positive and negative. The contactor was being touched only when the finger velocity was positive. The sinusoidal vibration of the contactor was largely maintained while it was being touched. The relative velocity is the difference between the finger velocity and that of the contactor

not be allowed to precisely discuss the occurrence of nominal sticking for which the relative velocity between the contact surfaces is zero. However, the friction force for 0.04-m/s condition was more zigzag than that for 0.1-m/s condition, indicating that the variation of friction caused by lateral vibration was more prominent when the finger velocity was smaller.

Unlike the simulation, the sticking did not occur at every cycle of the vibration of the contactor. Furthermore, the observed friction was always positive, defined as being in the direction of the finger motion. In the simulation previously mentioned in Fig. 7, the velocity of the contactor exceeded that of the finger, and the friction acted in the opposite direction of the finger movement; however, these phenomena were not observed in the experiments for every stimulus condition. In the simulation, we assumed that the finger and contactor exerted sufficient force to realize their intended or programmed motions. In the actual experiment, these assumptions did not hold mainly because of the external forces applied by the finger to the contactor system, which led to the discrepancies between the experiment and the simulation. In the phase in which the contactor was to exceed the finger, the finger pad and contactor could have stuck owing to the high level of friction.

Owing to the complex dynamics that were not modeled in this study, the variations in the actual friction were substantially more irregular than those in the simulation. Furthermore, although the participants were instructed to maintain a constant finger velocity and normal load, both actually varied during the course of the experiment.

The friction forces and relative velocities between the finger and contactor are extended in the time domain and shown in Fig. 12. The figure also shows those for the stationary contactor condition. Under this condition, the relative velocity was equal to that of the finger, and the friction force was relatively smooth. In contrast, when the relative velocity varied near zero for the finger velocity of 0.04 m/s, the transient changes of friction were prominent. The instantaneous drop of the relative velocity caused instantaneous change of the friction forces. When the instructed finger velocity was 0.1 m/s and greater than that of the contactor, the transient changes in friction were moderate.

Discussion

We hypothesized a principle for determining the degree of friction perceived when touching a vibrating contactor by considering two cases. The first was the case where the relative velocity between the fingertip and contactor is constantly positive, while the second was the case where the relative velocity can be zero. The results of a simulation based on this principle and psychophysical

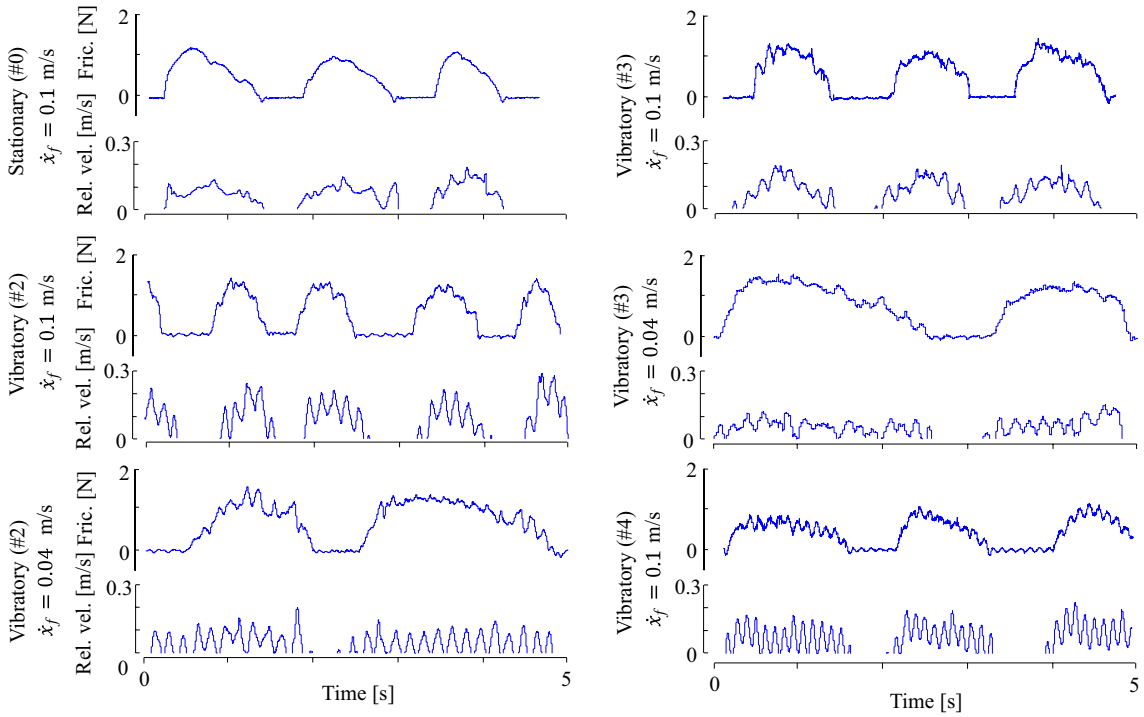

Fig. 12 Examples of friction forces and relative velocities between the finger nail and contactor. Those for stimulus #2 are from Fig. 11 for comparison

experiments were in good agreement. The principle of the hypothesis is that the friction temporarily increases owing to the decrease in the relative velocity between the sliding finger and the vibrating contactor. Nevertheless, only a limited number of material and stimulus conditions were tested in our experiment, and a general conclusion has yet to be attained. Here, we discuss the possible principles of friction perception via laterally vibrating contactor and the limitations of our study.

Effects of transient changes in friction forces caused by lateral vibration on friction perception

As shown in Fig. 10 (top), the differences in the average friction forces can be a maximum of 0.1 N among the five types of stimuli, which was shown to be discernible by a fingertip in a previous psychophysical study [44]. Nevertheless, it is necessary to question whether such a minor difference in the average friction forces would yield a clear perceptual difference if the deviation in the friction were to be considerable. Furthermore, although the apparent coefficients of friction were increased by the lateral vibration of the contactor, the coefficients for stimuli #1–#4 may not be significantly different from each other. These statistical aspects were not enough to describe the friction reported in the psychophysical experiments.

Introspective reports by the participants described their own personal judgment criteria after the experiment, with most participants referring to a "sense of sticking" when touching the vibrating contactor. This "sense of sticking" is assumed to be a rapid variation in the friction force rather than literal physical sticking between the finger pad and the contactor. Such variations in the friction were prominent for the conditions where the participants ranked high in terms of the perceived friction, as shown in Fig. 10 (middle). Based on these reports, it is reasonable to speculate that a temporal variation in the friction force caused by the change in the relative velocity might have led to the increase in the perceived friction. In other words, the increased perception may be in part due to the perceptive properties of humans to rapidly deviating friction forces rather than an increase in the average friction or coefficient of friction.

Conditions causing lateral vibration to increase friction perception

It should be noted that our experiment was conducted under limited conditions whereas various factors could influence a tribosystem. Here, the effects of these factors are discussed.

A critical factor that could influence our experiment is the surface roughness of the contactor material. In our experiment, the surface was smoothly finished. The surface roughness and friction are closely related [45, 46]. Because of the interlocking effects, surfaces with significant roughness develop large friction forces with a fingertip. On such surfaces, the finger frequently sticks and barely slides. Hence, our approach, in which the relative sliding velocity between the finger and contactor is manipulated with the intention of increasing the friction forces, would not function for contactors with large amounts of friction. Such an increase in friction also arises as a result of sweat [47]. Similarly, in the case of large contact forces (which were limited to approximately 1 N in the present study), the friction rises and the principle of our lateral vibration approach may not hold. In summary, when the surface friction is large enough to prevent the fingertip from smoothly sliding on the contactor, the effect of lateral vibrations is not expected.

The mutual effects of roughness and friction perception may also be a considerable factor. The roughness and friction perceptions influence each other [1, 48, 49]. In the case of materials with microscopic surface roughness, any relative motion between the finger and material give rise to the perception of roughness [50–52]. Hence, any change in the relative velocity between the fingertip and contactor, caused by a lateral vibration, potentially affects the perception of friction through roughness perception; such a mechanism is not considered in our hypothetical principles.

The vibratory frequency and finger velocity are also significant factors that could affect friction perception. The tested vibratory frequencies were within a range of 3 to 9 Hz, and the perceived friction increased with this frequency. However, at much higher frequencies, the cycle of the variation in $\dot{x}_r$ shortens, and the finger pad and contactor become less likely to stick. Hence, the perceived friction should not monotonically increase with a frequency higher than that tested in the present study. Furthermore, to attain an effective increase in the degree of friction, the finger velocity should be kept within an appropriate range. Based on our hypothesis, when the finger and contactor velocities are close and their relative velocity is small, a greater degree of friction is sensed. A method for controlling the velocity of the contactor according to the finger velocity would realize a more effective friction presentation.

Finally, the perception of friction via a laterally vibrotactile stimulus clearly depends on the difference between the coefficients of static and kinetic friction. The larger difference between these two types of friction is more likely to cause stick and slip phenomena. Hence, although we used finely polished ABS plastic, the use of more appropriate materials could lead to a more prominent perception of friction.

Conclusion

When a fingertip slides on a contactor that is vibrating in the lateral direction at a low frequency with an amplitude of approximately 1 mm, a larger friction is perceived than when sliding on a stationary contactor [30, 31]. This phenomenon is expected to be exploited in new types of vibrotactile displays. As part of our investigation of the perception principle, we hypothesized that the perceived friction increases owing to a stick and slip phenomenon and the Stribeck characteristic when the relative velocity between the fingertip and contactor is low. We measured the tangential and normal interaction forces between the finger and contactor using an instrumented lateral vibrotactile display. Based on the measured friction and finger motion, we simulated friction acting on a finger sliding on a vibrating contactor. We then recruited five participants and performed psychophysical experiments on friction perception. The results of the friction simulation, psychophysical experiments and measured friction during the experiments suggested that the transient increases in friction caused by the decrease in the relative velocity influenced friction perception for the vibrating contactor, indicating that our hypothetical principle can be one explanation of the observed phenomena. In particular, among the tested conditions, the largest degree of friction was perceived when touching the contactor vibrating at 6 or 9 Hz with an amplitude of 1.25 mm. From another aspect, a greater degree of friction was perceived when the relative velocities between the finger and contactor temporarily approach zero. These facts indicate that an effective friction display could be achieved by controlling the velocity of a vibrating contactor in response to being touched by a finger.

Authors' contributions

AI and SO are the main contributors of this study, including formulating the concepts and principles, conducting experiments and analyses, and editing the manuscript. YY is credited with the principles of the methods. All authors have read and approved the final manuscript

Acknowledgements

This study was partly supported by MIC SCOPE (142106003).

Competing interests

The authors declare that they have no competing interests.

Publisher's Note

Springer Nature remains neutral with regard to jurisdictional claims in published maps and institutional affiliations.

Received: 18 May 2016 Accepted: 14 April 2017
Published online: 24 April 2017

References

1. Fagiani R, Massi F, Chatelet E, Berthier Y, Akay A (2011) Tactile perception by friction induced vibrations. Tribol Int 44(10):1100–1110
2. Nonomura Y, Fujii T, Arashi Y, Miura T, Maeno T, Tashiro K, Kamikawa Y, Monchi R (2009) Tactile impression and friction of water on human skin. Colloids Surf B Biointerfaces 69(2):264–267
3. Smith AM, Chapman CE, Deslandes M, Langlais J-S, Thibodeau M-P (2002) Role of friction and tangential force variation in the subjective scaling of tactile roughness. Exp Brain Res 144(2):211–223
4. Derler S, Süess J, Rao A, Rotaru G-M (2013) Influence of variations in the pressure distribution on the friction of the finger pad. Tribol Int 63:14–20
5. Nakano K (2008) Information regarding tactile sensation in friction signals with high uncertainty. Tribol Int 41(11):1114–1125
6. Kim M-S, Kim I-Y, Park Y-K, Lee Y-Z (2013) The friction measurement between finger skin and material surfaces. Wear 301(1):338–342
7. Murphy TE, Webster III RJ, Okamura AM (2004) Design and performance of a two-dimensional tactile slip display. In: Proceedings of the EuroHaptics, Munich, pp 130–137
8. Provancher WR, Sylvester ND (2009) Fingerpad skin stretch increases the perception of virtual friction. IEEE Trans Haptics 2(4):212–223
9. Matsui K, Okamoto S, Yamada Y (2014) Amplifying shear deformation of finger pad increases tracing distances. Adv Robot 28(13):883–893
10. Matsui K, Okamoto S, Yamada Y (2014) Relative contribution ratios of skin and proprioceptive sensations in perception of force applied to fingertip. IEEE Trans Haptics 7(1):78–85
11. Yamamoto A, Nagasawa S, Yamamoto H, Higuchi T (2006) Electrostatic tactile display with thin film sliderand its application to tactile telepresentation systems. IEEE Trans Vis Comput Graph 12(2):168–177
12. Bau O, Poupyrev I, Israr A, Harrison C (2010) Teslatouch: electrovibration for touch surfaces. In: Proceedings of Annual ACM Symposium on User Interface Software and Technology, New York, pp 283–292
13. Chubb EC, Colgate JE, Peshkin MA (2010) ShiverPaD: a glass haptic surface that produces shear force on a bare finger. IEEE Trans Haptics 3(3):189–198
14. Biet M, Boulon L, Martinot F, Giraud F, Lemaire-Semail B (2007) Using an ultrasonic transducer: evidence for an anisotropic deprivation of frictional cues in microtexture perception. In: Proceedings of IEEE World Haptics Conference, Tsukuba, pp 385–390
15. Takasaki M, Nara T, Tachi S, Higuchi T (2000) A tactile display using surface acoustic wave. In: Proceedings of IEEE international workshop on robot and human interactive Communication, Osaka, pp 364–367
16. Konyo M, Yamada H, Okamoto S, Tadokoro S (2008) Alternative display of friction represented by tactile stimulation without tangential force. In: Ferre M (ed) Haptics: perception, devices and scenarios. Springer, Berlin, pp 619–629
17. Yamauchi T, Okamoto S, Konyo M, Tadokoro S (2010) Real-time remote transmission of multiple tactile properties through master-slave robot system. In: Proceedings of IEEE international conference on robotics and automation, Anchorage, pp 1753–1760
18. Konyo M, Yoshida A, Tadokoro S, Saiwaki N (2005) A tactile synthesis method using multiple frequency vibration for representing virtual touch. In: Proceedings of IEEE/RSJ international conference on intelligent robots and systems, Edmonton, pp 3965–3971
19. Asano S, Okamoto S, Yamada Y (2014) Toward quality texture display: vibrotactile stimuli to modify material roughness sensations. Adv Robot 28(16):1079–1089
20. Caldwell DG, Gosney C (1993) Multi-modal tactile sensing and feedback (tele-taction) for enhanced tele-manipulator control. In: Proceedings of IEEE/RSJ international conference on intelligent robots and systems, Yokohama, pp 1487–1494
21. Culbertson H, Unwin J, Kuchenbecker KJ (2014) Modeling and rendering realistic textures from unconstrained tool-surface interactions. IEEE Trans Haptics 7(3):381–393
22. Saga S, Raskar R (2013) Simultaneous geometry and texture display based on lateral force for touchscreen. In: Proceedings of the IEEE world haptics conference, Istanbul, pp 437–442
23. Okamura AM, Cutkosky MR, Dennerlein JT (2001) Reality-based models for vibration feedback in virtual environments. IEEE/ASME Trans Mechatron 6(3):245–252
24. Kuchenbecker KJ, Fiene J, Niemeyer G (2006) Improving contact realism through event-based haptic feedback. IEEE Tran Vis Comput Graph 12(2):219–230
25. Higashi K, Okamoto S, Yamada Y (2015) Effects of mechanical parameters on hardness experienced by damped natural vibration stimulation. In: Proceedings of IEEE international conference on systems, man, and cybernetics, HongKong, pp 1539–1544
26. Ikeda Y, Hasegawa S (2009) Characteristics of perception of stiffness by varied tapping velocity and penetration in using event-based haptic. In: Proceedings of joint virtual reality eurographics conference on virtual environments, Lyon, pp 113–116
27. Lang J, Andrews S (2011) Measurement-based modeling of contact forces and textures for haptic rendering. IEEE Trans Vis Comput Graph 17(3):385–391
28. Visell Y, Okamoto S (2014) Vibrotactile sensation and softness perception. In: Luca MD (ed) Multisensory softness. Springer, Berin, pp 31–48
29. Ben Porquis L, Konyo M, Tadokoro S (2011) Representation of softness sensation using vibrotactile stimuli under amplitude control. In: Proceedings of the IEEE international conference on robotics and automation, pp 1380–1385
30. Imaizumi A, Okamoto S, Yamada Y (2014) Friction sensation produced by laterally asymmetric vibrotactile stimulus. In: Auvray M, Duriez C (eds) Haptics: neuroscience, devices, modeling, and applications, part II, vol 8619., Lecture notes in computer scienceSpringer, Berlin, pp 11–18
31. Imaizumi A, Okamoto S, Yamada Y (2015) Friction perception by laterally vibrotactile stimulus: early demonstration. In: Kajimoto H, Ando H, Kyung K-U (eds) Haptic interaction: perception, devices and applications, vol 277., Lecture notes in electrical engineeringSpringer, Berlin, pp 113–117
32. Wiertlewski M, Hayward V (2012) Mechanical behavior of the fingertip in the range of frequencies and displacements relevant to touch. J Biomech 45(11):1869–1874
33. Nakazawa N, Ikeura R, Inooka H (2000) Characteristics of human fingertips in the shearing direction. Biol Cybern 82(3):207–214
34. Derler S, Rotaru G-M (2013) Stick-slip phenomena in the friction of human skin. Wear 302(1–2):324–329
35. Persson BNJ, Kovalev A, Gorb SN (2012) Contact mechanics and friction on dry and wet human skin. Tribol Lett 50(1):17–30
36. Mahdi D, Riches A, Gester M, Yeomans J, Smith P (2015) Rolling and sliding: separation of adhesion and deformation friction and their relative contribution to total friction. Tribol Int doi:10.1016/j.triboint.2014.12.021
37. Greenwood JA, Tabor D (1957) The friction of hard sliders on lubricated rubber: the importance of deformation losses. Proc Phys Soc 71:989–1001
38. Adams MJ, Briscoe BJ, Johnson SA (2007) Friction and lubrication of human skin. Tribol Lett 26(3):239–253
39. Terekhov AV, Hayward V (2011) Minimal adhesion surface area in tangentially loaded digital contacts. J Biomech 44(13):2508–2510
40. Morley JW, Goodwin AW, Darian-Smith I (1983) Tactile discrimination of gratings. Exp Brain Res 49:291–299
41. Smith A, Gosselin G, Houde B (2002) Deployment of fingertip forces in tactile exploration. Exp Brain Res 147(2):209–218
42. Yoshioka T, Bensmaïa SJ, Craig JC, Hsiao SS (2007) Texture perception through direct and indirect touch: an analysis of perceptual space for tactile textures in two modes of exploration. Somatosens Motor Res 24(1–2):53–70
43. Scheffe H (1952) An analysis of variance for paired comparisons. J Am Stat Assoc 47(259):381–400
44. Paré M, Carnahan H, Smith AM (2002) Magnitude estimation of tangential force applied to the fingerpad. Exp Brain Res 142:342–348
45. Derler S, Gerhardt LC (2012) Tribology of skin: review and analysis of experimental results for the friction coefficient of human skin. Tribol Lett 45:1–27
46. van Kuilenburg J, Masen MA, van der Heide E (2015) A review of fingerpad contact mechanics and friction and how this affects tactile perception. Proc Inst Mech Eng J J Eng Tribol 229(3):243–258
47. Adams MJ, Johnson SA, Lefèvre P, Lévesque V, Hayward V, André T, Thonnard J-L (2013) Finger pad friction and its role in grip and touch. J R Soc Interface 10:20120467

48. Chen X, Barnes CJ, Childs THC, Henson B, Shao F (2009) Materials' tactile testing and characterization for consumer products' affective packaging design. Mater Design 30:4299–4310
49. Smith AM, Basile G (2010) Roughness of simulated surfaces examined with a haptic tool: effects of spatial period, friction, and resistance amplitude. Exp Brain Res 202(1):33–43
50. Bensmaïa SJ, Hollins M (2003) The vibrations of texture. Somatosens Motor Res 20(1):33–43
51. Lederman SJ (1974) Tactile roughness of grooved surfaces: the touching process and effects of macro-and microsurface structure. Percept Psychophys 16(2):385–395
52. Meftah EM, Belingard L, Chapman CE (2000) Relative effects of the spatial and temporal characteristics of scanned surfaces on human perception of tactile roughness using passive touch. Exp Brain Res 132(3):351–361

Submit your manuscript to a SpringerOpen journal and benefit from:

► Convenient online submission
► Rigorous peer review
► Immediate publication on acceptance
► Open access: articles freely available online
► High visibility within the field
► Retaining the copyright to your article

Submit your next manuscript at ► springeropen.com